Mixing across the Arctic Ocean: Microstructure observations during the Beringia 2005 Expedition

Luc Rainville[1] and Peter Winsor[2]

Received 6 February 2008; accepted 27 March 2008; published 30 April 2008.

[1] Turbulent-scale temperature and conductivity were measured during the pan-arctic Beringia 2005 Expedition. The rates of dissipation of thermal variance and diapycnal diffusivities are calculated along a section from Alaska to the North Pole, across deep flat basins (Canada and Makarov Basins) and steep ridges (Alpha-Mendeleev and Lomonosov Ridges). The mixing rates are observed to be small relative to lower latitudes but also remarkably non-uniform. Relatively elevated turbulence is found over deep topography, confirming the dominant role of bottom-generated internal waves. Measured patterns of mixing in the Arctic are also associated with other mechanisms, such as double-diffusive structures and deep overflows. A better knowledge of the distribution of mixing is essential to understand the dynamics of the changing Arctic environment. **Citation:** Rainville, L., and P. Winsor (2008), Mixing across the Arctic Ocean: Microstructure observations during the Beringia 2005 Expedition, *Geophys. Res. Lett.*, *35*, L08606, doi:10.1029/2008GL033532.

1. Introduction

[2] The Arctic Ocean plays important role in climate dynamics and is a sensitive indicator of climate change [*Holloway and Proshutinsky*, 2007]. As such, our ability to understand the present climate system and to predict its likely response to altered forcing may hinge on our knowledge of the Arctic Ocean circulation and mixing.

[3] The Arctic Ocean is characterized by strong upper-ocean stratification, double-diffusive layers and intrusions, and by relatively isolated deep waters with well-mixed homogenous bottom layers. Mixing rates, mixing geography and processes are largely unknown. Slightly elevated levels of upper ocean turbulence have been measured in association with a shallow halocline eddy in the Canada Basin [*Padman et al.*, 1990], and only a few studies have investigated mixing near major topographical features of the Arctic Ocean like the Yermak Plateau [*Padman and Dillon*, 1991] and in its marginal seas [*Sundfjord et al.*, 2007]. Previous studies, mostly based on data from the Eastern Arctic, also noted a correlation between bottom topography and internal wave shear, suggesting that mixing is related to bottom topography [*D'Asaro and Morison*, 1992; *Dewey et al.*, 1999].

[4] During the Beringia 2005 Expedition, the Swedish icebreaker *Oden* and the United States Coast Guard Cutter *Healy* completed a transect across the Arctic Ocean [*Björk et al.*, 2007]. In addition to the full physical and biogeochemical hydrographic program, we used a Vertical Microstructure Profiler (VMP, built by Rockland Scientific International) to measure turbulence-scale temperature, conductivity, and shear, as well as obtain high-resolution conductivity-temperature-depth (CTD) profiles. In total, we collected 23 VMP casts at 16 different locations (Figure 1). As far as we know, this is the first basin-scale direct survey of turbulence in the Arctic. The data confirm the low level of turbulence suggested by past finescale (meter-scale) velocity and density measurements and reveal a strong spatial variability remarkably linked to bottom topography.

2. Measurements

[5] The VMP is smaller and more streamlined than a CTD rosette, creating much less water disturbance, providing higher vertical resolution, as well as faster and easier deployments. Because of nearly 100% ice cover conditions and the fact that the microstructure program was on an opportunity basis during Beringia, we chose to use the ship winch and power the instrument with a regular conducting wire cable, lowering it at a nearly constant speed (between 0.95 and 1.05 m s^{-1}). Data were recorded internally and downloaded after each recovery. The winch and the wire rope induce vibrations, which were somewhat damped by adding a pinger a few meters above the instrument (acting strictly as a weight, since we found that the pings affected the VMP electronics) and by decoupling the instrument from the wire rope with a bungee cord.

[6] The VMP is equipped with six microstructure probes located in the nose cone (2 fast-response thermistors [FP07], 2 micro-conductivity probes [SBE-7] and 2 velocity shear probes [SPM1-38]) together with a pumped SBE-9 CTD and three-axis accelerometers to track instrument vibrations. In order to increase sampling resolution, data from the microstructure sensors are recorded at 512 Hz as the signal plus its derivative [*Mudge and Lueck*, 1994]. Because of the configuration we used, the signal from the shear probes is noisy and questionable, therefore not adequate to estimate kinetic energy diffusivity. The micro-temperature and micro-conductivity measurements, on the other hand, reveal new and significant patterns of turbulence in the Arctic.

[7] To reduce salinity spiking, the response of the conductivity sensor was matched to that of the temperature sensor by finding the time and thermal response lags of the sensors [*Ferrari and Rudnick*, 2000]. The high resolu-

[1]Applied Physics Laboratory, University of Washington, Seattle, Washington, USA.
[2]Physical Oceanography Department, Woods Hole Oceanographic Institution, Woods Hole, Massachusetts, USA.

0094-8276/08/2008GL033532$05.00

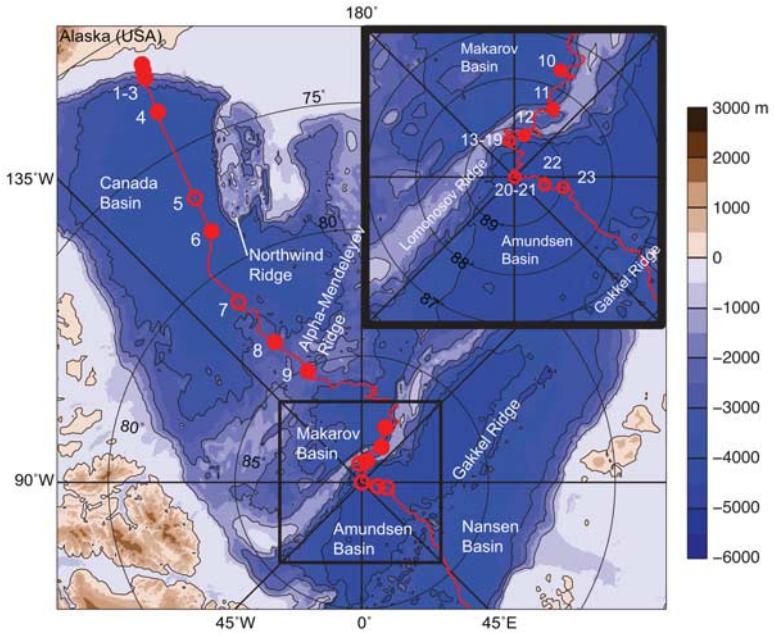

Figure 1. Locations of the microstructure profiles during the Beringia 2005 Expedition. Filled circles indicate the full-depth VMP profiles and open circles the profiles to 1000 m. Red line is the icebreaker Oden cruise track. The colormap shows the bathymetry.

tion of the CTD data enables us to look at the detailed structure of the water column at ~2 Hz (vertical scale of ~0.5 m) while the microstructure data can be resolved at a vertical scales of 2–3 cm.

3. Results

[8] Microstructure profiles were recorded from the Alaska continental shelf to the Amundsen Basin, across the North Pole (Figure 1). The full-water column potential temperature and salinity profiles for cast #11 are plotted in Figure 2a. This station illustrates well the quality of the data. Co-located with Beringia station #35, this site is on the Lomonosov Ridge at 88°24.8′N, 150°33.1′E. Fourier spectra of microstructure potential temperature gradient (Figure 2b) are calculated for each 2-sec block of data, using 8 degrees of freedom (256 points). For each of these blocks the variance of the temperature gradient is calculated by integrating the spectrum up to the frequency where noise becomes dominant, which is determined by comparing the shape of the spectrum with that of the electronic noise (Figure 2d, dashed line), or to an ad-hoc value of 70 Hz. These criterion are somewhat equivalent to trying to fit the turbulence Batchelor spectrum [*Batchelor*, 1959] to the temperature gradient spectrum, but we preferred not to make any a priori assumptions.

[9] The rate of dissipation of thermal variance is estimated from isotropic turbulence theory as being $\chi = 6D\ \langle\theta_z^2\rangle$, where the molecular diffusivity, D, is equal to 1.4×10^{-7} m^2 s^{-1} for cold temperatures, and $\langle\theta_z^2\rangle$ is the variance of the vertical gradient of potential temperature, calculated over a 2-sec window [*Roget et al.*, 2006]. The relatively high fall rate is far from being optimal for micro-temperature measurements and the thermistor response for such conditions is questionable [*Gregg*, 1999]. However some confidence in the results is provided by the fact that independent χ estimates based on micro-conductivity are always within a factor of 2 from those from micro-temperature (Figure 2c). Micro-conductivity estimates are calculated assuming that the majority of the fluctuations in conductivity are associated to temperature fluctuations (as opposed to salinity) and therefore scaling the conductivity gradient signal by 1.11 K m S^{-1} [*Klymak et al.*, 2008]. The noise floor is higher for micro-conductivity measurements - the minimum 50-m χ value from micro-conductivity seems to be around 2×10^{-11} K^2 s^{-1} relative to less than 5×10^{-12} K^2 s^{-1} for micro-temperature estimates.

[10] The rate of dissipation of thermal variance versus depth for cast #11 is plotted in Figure 2c. High values of the rate of turbulent dissipation are seen between 100 and 200-m, and large patches of enhanced rate of dissipation are seen below 1200 m. The total water depth at this station is 1870 m. It is located at the lowest point of the Lomonosov Ridge crest (regionally), flanked on either side - 10 to 25 km away - by topographic features with depths of about 1200 m [*Björk et al.*, 2007]. The deep turbulence signal observed near station 11 is likely due to the water exchange between the Makarov and Amundsen Basis, documented by *Björk et al.* [2007]. The dynamics of such an overflow, and even its direction, are far from being clear: *Timmermans et al.* [2005] suggested the presence of a deep flow from the Amundsen Basin towards the Makarov Basin, while further analysis by *Timmermans and Garrett* [2006] indicates a much smaller flow, and the Beringia 2005 observations suggest the opposite direction [*Björk et al.*, 2007].

[11] The rate of dissipation of thermal variance along a section across the Arctic Ocean, from the Alaska shelf to the North Pole, is shown in Figure 3. Depth-averaged rates are shown in Figure 3 (bottom).

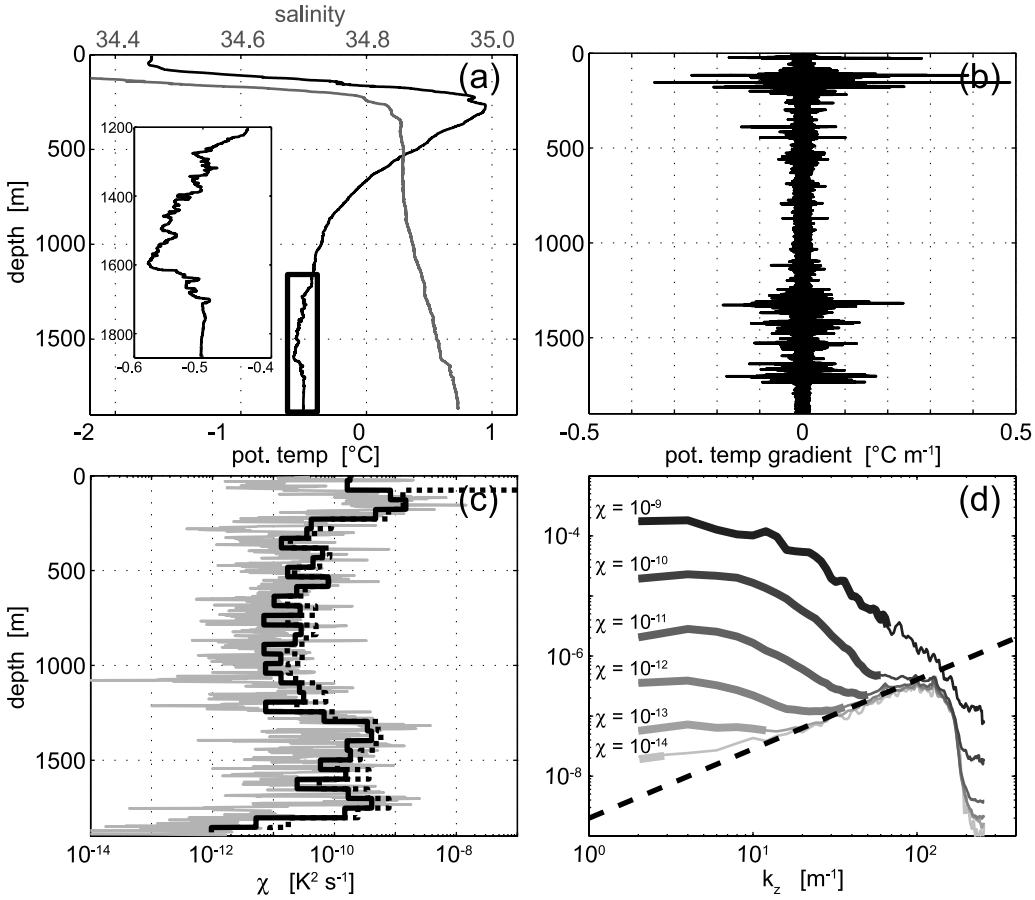

Figure 2. (a) Potential temperature and salinity profiles at station 11, located: on the Lomonosov Ridge. Inset shows the potential temperature profile below 1200 m. (b) Microstructure profile of potential temperature gradient. (c) 2-sec estimate (gray) and 50-m average rate of dissipation of thermal variance χ from temperature (black) and conductivity (dotted). (d) Temperature gradient spectra for that profile, binned by their value of χ. The top line shows the average spectrum for all the 2-sec ensembles that have a rate of dissipation of thermal variance higher than 10^{-9} K^2 s^{-1} and so on down to 10^{-14} K^2 s^{-1}. Range of integration for the variance is indicated by the thick line. Units for the power spectral density are (K m^{-1})^2/cpm. An estimate of the electronic noise (micro-temperature signal in quiescent water) is shown in dashed.

[12] In the upper ocean (100–400 m), the highest dissipation rates are found on the Alaska shelf (stations 1–3). Most of the other stations also have large values of χ in the upper 500 m, generally associated with the sharp temperature increase associated with the top of the Atlantic water (typically between 200 and 300 m). These rates are slightly higher over the Lomonosov Ridge (stations 12 and 13), about 3 times that of stations 5 to 10 ($\sim 2 \times 10^{-10}$ K^2 s^{-1}). The lowest upper ocean dissipation values are found at station 4, located the farthest away from any topographic features. Stations 5 and 6 are also in the Canada Basin interior, but relatively close to the Northwind Ridge. The large intrusions seen in the upper 200 m at station 6, likely associated with the structures described by *Woodgate et al.* [2007], are associated with rate of dissipation of thermal variance of the order of 10^{-9} K^2 s^{-1}.

[13] Between 1300 and 1800 m, the stations in the interior and near the Alpha-Mendeleev Ridge (stations 4, 6, and 8) all have $\chi \sim 10^{-12}$ K^2 s^{-1}. The dissipation at station 9, near the crest of the ridge, is only slightly higher (3×10^{-12} K^2 s^{-1}). The highest deep dissipation rates are found at station 11, on the flanks of the Lomonosov Ridge, where values are well above those found between 500–1000 m. At station 11, the values of χ around 1500 m are comparable to those seen in the upper 200 m.

4. Discussion

[14] Unfortunately, the microstructure shear data are not clean enough to obtain meaningful estimates of the rate of turbulent kinetic energy dissipation (ε). Turbulent levels in the Arctic Ocean are low, and our attempts to fit the Bachelor spectrum to the micro-temperature (or micro-conductivity) gradient spectra to estimate the rates of dissipation of both turbulent kinetic energy and thermal variance [*Ruddick et al.*, 2000; *Luketina and Imberger*, 2001] have not, so far, provided solid estimates.

[15] Temperature diffusivity K_T can be estimated from χ using $K_T = \chi/2(\partial\theta/\partial z)^2$. The estimated profile of K_T for the top 1000 m of station 11 is shown in Figure 4c. It is often assumed that turbulence results in the same Fickian diffusion of temperature and density, therefore interpreting K_θ as a diapycnal diffusivity (K_ρ). The validity of this assumption in the presence of intrusions or for regions of very low stratification (as in the deep Arctic) is doubtful.

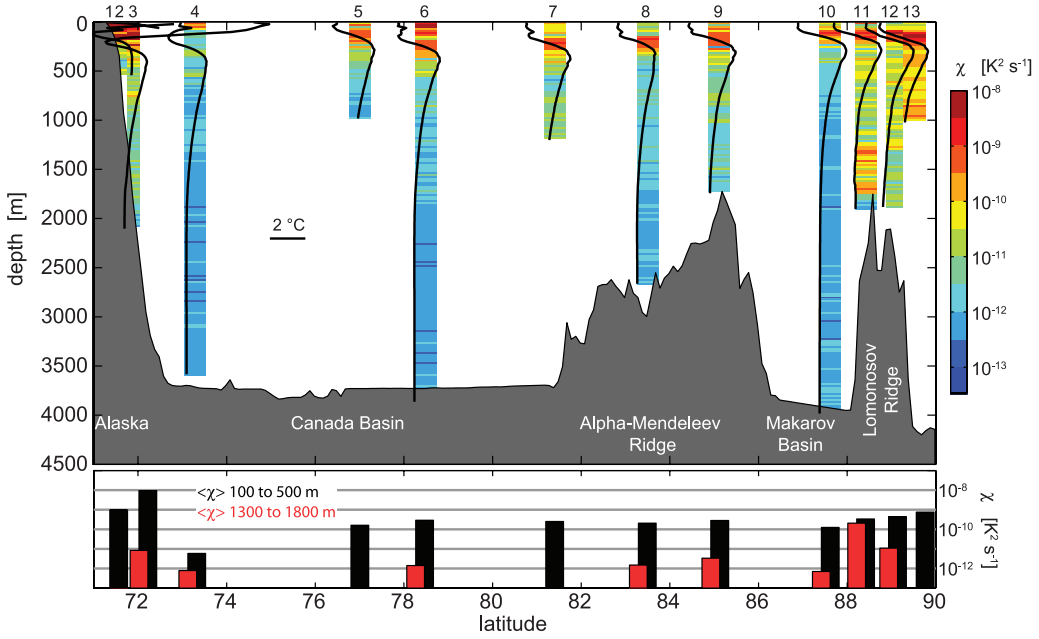

Figure 3. Top panel: Rate of dissipation of thermal variance across a section of the Arctic Ocean, from microstructure temperature profiles (color). The potential temperature profile at each station is plotted as the black line (scale is shown in black, 0°C centered on the center of the color bar. Bathymetry is shown in gray and casts number are labeled on the top axis. Bottom panel: Averaged rate of dissipation of thermal variance - on a logarithmic scale - from 100 to 500 m (black), and 1300 to 1800 m (red).

[16] In addition to using microstructure, density profiles can be used to detect overturns and estimate ε [*Thorpe*, 1977]. For each density inversion in the potential density profile, a Thorpe length L_ρ is defined as the distance by which a water parcel has to be moved to restore stability (sorted profile). Using the overall stratification across each overturn, N_T, the turbulence dissipation rate for each overturn (Figure 4b) can be estimated as $\varepsilon \approx L_\rho^2 N_T^2$ (see *Klymak et al.* [2008] for details). The dissipation rates can in turn be converted to density diffusivity K_ρ using the Osborn-Cox assumption: $K_\rho = \Gamma\varepsilon/N^2$, with the mixing efficiency Γ taken as being 0.2.

[17] Both independent methods lead to similar estimates (Figure 4). Overall, the elevated values of χ observed in the upper ocean correspond to diffusivity values of $O(10^{-5})$ m^2 s^{-1}, much smaller than at mixing hot-spots observed near seamounts and ridges at lower latitudes [e.g., *Lueck and Mudge*, 1997; *Rudnick et al.*, 2003]. In the deeper ocean and interior basins, diffusivity values estimated from microstructure or Thorpe scales are $O(10^{-6})$ m^2 s^{-1} and lower (not shown). *Polzin et al.* [1997], in contrast, measured diffusivities ranging from $<10^{-5}$ to 10^{-3}m^2 s^{-1} in the deep Brazil Basin. It is important to keep in mind that diffusivities calculated by Thorpe scale analysis from single profiles might not be very accurate. Repeated profiles and a careful analysis of noise and of the overturn statistics are called for.

[18] The microstructure data collected during Beringia 2005 show that there is an measurable turbulence signal both along the boundaries and in the interior of the Arctic Ocean. Overall mixing rates are found to be small compared to other oceans and highly non-uniform. Because of its

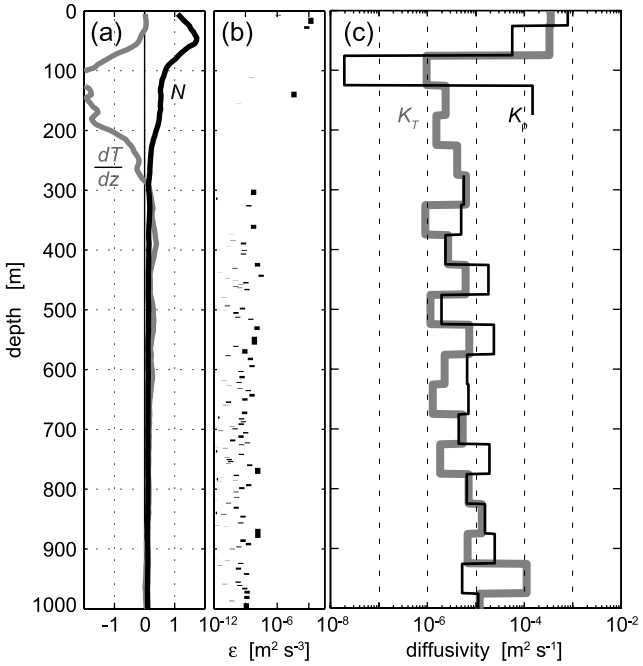

Figure 4. Station # 11: (a) Profiles of potential temperature gradient (gray, in units of 10^{-2} K m^{-1}) and buoyancy frequency (black, in units of 10^{-2} rad s^{-1}). (b) Turbulent dissipation rate ε from each density overturn. (c) Isopycnal diffusivity profile calculated from χ (K_T, thick gray) and from density overturns ($K\rho$, black).

relation with deep topography, much of the observed turbulence appears to be associated with internal waves generated by flow over topography, as suggested by [*D'Asaro and Morison*, 1992], emphasizing the importance of the weak Arctic tides. Near-inertial waves generated by ice-pack motion must also play a important role in controlling mixing rates in the Arctic [*Pinkel*, 2005], but our sparse observations are not sufficient to confirm this.

[19] The enhanced dissipation rates observed above the Atlantic Water layer throughout the Western Arctic during Beringia 2005 is likely to be associated with the double-diffusive staircase and intrusions often observed in that water mass [*Woodgate et al.*, 2007]. The role of those structures to transport heat and salt is still very much an open question. It is also quite unclear if the mixing parameterizations developed and used in the mid-latitudes are valid for the Arctic Ocean.

[20] As the ice cover continues to decline, it is reasonable to assume that increased near-inertial waves generated at the surface will enhanced shear and mixing across the Arctic. Stronger and more uniform turbulence will drastically change the properties and dynamics of the Arctic Ocean. From both modeling and observational perspectives, the unique magnitude and spatial variability of diapycnal mixing have to be taken into account to understand the current and future dynamics of the Arctic Ocean. Detailed microstructure measurements are essential to further this effort.

[21] **Acknowledgments.** We are grateful to the crew of icebreaker Oden for their professional help during Beringia 2005, to the Swedish Polar Research Secretariat for logistics and planning, and to all the expedition participants for their support during the cruise. We thank Mary-Louise Timmermans and the reviewers for their constructive comments. This work was funded by the National Science Foundation through a Small Grant for Exploratory Research (ARC-0527874) and grant ARC-0612342 with additional support from the Doherty Foundation and internal WHOI Funds.

References

Batchelor, G. (1959), Small-scale variation of convected quantities like temperature in turbulent fluid, *J. Fluid Mech.*, *5*, 113–133.

Björk, G., et al. (2007), Bathymetry and deep-water exchange across the central Lomonosov Ridge at 88°–89°N, *Deep Sea Res., Part I*, *54*, 1197–1208.

D'Asaro, E. A., and J. H. Morison (1992), Internal waves and mixing in the Arctic Ocean, *Deep Sea Res., Part A.*, *39*, S459–S484.

Dewey, R., R. Muench, and J. Gunn (1999), Mixing and vertical heat flux estimates in the Arctic Eurasian Basin, *J. Mar. Syst.*, *21*, 199–205.

Ferrari, R., and D. L. Rudnick (2000), Thermohaline variability in the upper ocean, *J. Geophys. Res.*, *105*, 16,857–16,883.

Gregg, M. C. (1999), Uncertainties and limitations in measuring ε and χ_T, *J. Atmos. Oceanic Technol.*, *16*, 1483–1490.

Holloway, G., and A. Proshutinsky (2007), Role of tides in Arctic ocean/ice climate, *J. Geophys. Res.*, *112*, C04S06, doi:10.1029/2006JC003643.

Klymak, J. M., R. Pinkel, and L. Rainville (2008), Direct breaking of the internal tide near topography: Kaena ridge, Hawaii, *J. Phys. Oceanogr.*, *38*, 380–399.

Lueck, R. G., and T. D. Mudge (1997), Topographically induced mixing around a shallow seamount, *Science*, *276*, 1831–1833.

Luketina, D. A., and J. Imberger (2001), Determining turbulent kinetic energy dissipation from Batchelor curve fitting, *J. Atmos. Oceanic Technol.*, *18*, 100–113.

Mudge, T. D., and R. G. Lueck (1994), Digital signal processing to enhance oceanographic observations, *J. Atmos. Oceanic Technol.*, *11*, 825–836.

Padman, L., and T. Dillon (1991), Turbulent mixing near the Yermak Plateau during the Coordinated Eastern Arctic Experiment, *J. Geophys. Res.*, *96*, 4769–4782.

Padman, L., M. D. Levine, T. Dillon, J. Morison, and R. Pinkel (1990), Hydrography and microstructure of an arctic cyclonic eddy, *J. Geophys. Res.*, *95*, 9411–9420.

Pinkel, R. (2005), Near-inertial wave propagation in the western Arctic, *J. Phys. Oceanogr.*, *35*, 645–665.

Polzin, K. L., J. M. Toole, J. R. Ledwell, and R. W. Schmitt (1997), Spatial variability of turbulent mixing in the abyssal ocean, *Science*, *276*, 93–96.

Roget, E., I. Lozovatsky, X. Sanchez, and M. Figueroa (2006), Microstructure measurements in natural waters: Methodology and applications, *Prog. Oceanogr.*, *70*, 126–148.

Ruddick, B., A. Anis, and K. Thompson (2000), Maximum likelihood spectral fitting: The Batchelor spectrum, *J. Atmos. Oceanic Technol.*, *17*, 1541–1555.

Rudnick, D. L., et al. (2003), From tides to mixing along the Hawaiian Ridge, *Science*, *301*, 355–357.

Sundfjord, A., I. Fer, Y. Kasajima, and H. Svendsen (2007), Observations of turbulent mixing and hydrography in the marginal ice zone of the Barents Sea, *J. Geophys. Res.*, *112*, C05008, doi:10.1029/2006JC003524.

Thorpe, S. A. (1977), Turbulence and mixing in a Scottish Loch, *Philos. Trans. R. Soc. London, Ser. A*, *286*, 125–181, doi:10.1098/rsta.1977.0112.

Timmermans, M.-L., P. Winsor, and J. A. Whitehead (2005), Deep-water flow over the Lomonosov Ridge in the Arctic Ocean, *J. Phys. Oceanogr.*, *35*, 1489–1493.

Timmermans, M.-L., and C. Garrett (2006), Evolution of the deep water in the Canadian Basin in the Arctic Ocean, *J. Phys. Oceanogr.*, *36*, 866–874.

Woodgate, R. A., K. Aagaard, J. H. Swift, W. M. Smethie Jr., and K. K. Falkner (2007), Atlantic water circulation over the Mendeleev Ridge and Chukchi Borderland from thermohaline intrusions and water mass properties, *J. Geophys. Res.*, *112*, C02005, doi:10.1029/2005JC003416.

L. Rainville, Applied Physics Laboratory, University of Washington, Seattle, WA 98105-6698, USA. (rainville@apl.washington.edu)

P. Winsor, Physical Oceanography Department, Woods Hole Oceanographic Institution, Woods Hole, MA 02543, USA.